

Grooving of a grain boundary by evaporation–condensation below the roughening transition

H. A. Stone^{a)} and M. J. Aziz

Division of Engineering and Applied Sciences, Harvard University, Cambridge, Massachusetts 02138

D. Margetis

Department of Mathematics, Massachusetts Institute of Technology (MIT), Cambridge, Massachusetts 01239

(Received 23 September 2004; accepted 4 April 2005; published online 6 June 2005)

The development of surface grooves at grain boundaries that intersect a planar surface is analyzed for the case that the evolution occurs below the thermodynamic roughening transition by evaporation–condensation processes. The dynamics are described by a nonlinear partial differential equation that has a similarity solution, so the resulting groove profile is described by a nonlinear ordinary differential equation. An approximate analytical solution to the nonlinear problem is obtained and is in excellent agreement with the numerical solution. The depth and width of the groove varies as $t^{1/2}$, where t is time, analogous to the classical results valid above the thermodynamic roughening temperature. In addition, the approximate analytical solution provides an explicit relation between the groove width and the dihedral angle, and is in sufficiently good agreement with the numerical results as to make such numerical solutions unnecessary for this problem. The results demonstrate explicitly how the groove shape depends on the functional form of the slope-dependent surface mobility. © 2005 American Institute of Physics.

[DOI: 10.1063/1.1922583]

I. INTRODUCTION

Grain boundary grooving is an important factor in two-dimensional grain growth of thin films. The deepening of grain boundary grooves at the surface tends to pin the boundaries and impede grain growth, ultimately causing stagnation of the evolution.^{1–3} The morphological profile of the sloping sides is important because the local slope determines the driving force for grain growth required for the boundary to break free of the groove. The classical analysis for thermal grooving, with an isotropic surface free energy, by either surface diffusion or evaporation–condensation processes was provided by Mullins.⁴

Theoretical treatments of morphological evolution have been extended to anisotropic surface free energy,^{5,6} but have not included the singularity in surface free energy at the orientation of a facet. Particularly noteworthy is the treatment of Xin and Wong,⁵ who regularized the singularity by replacing it with an analytic approximation. This approach, however, when applied to the decay of a surface in the absence of grain boundaries,^{7,8} has drawn criticism^{9–11} (see also Ref. 12, p. 13707) and has been claimed not to correctly reproduce the evolution of facet edges.¹³ Recently, however, an approach based on partial differential equations (PDEs) has been developed,^{14,15} based on the singular surface free energy of Gruber and Mullins,¹⁶ that correctly predicts quantitative features of the evolution of facet edges, such as universal scaling with physical parameters, when compared to step-kinetic simulations.¹¹

Here we provide an analysis that treats grain-boundary

grooving and deals directly with the singularity in the surface free energy. We predict the deepening rate and the morphological profile of the sloping sides for a surface free-energy model appropriate for a grain boundary in a thin film exhibiting “fiber texture,” a common thin-film grain morphology in which the surface normal orientation of all grains is the same low-index direction, but neighboring grains are misoriented azimuthally. The method is valid for groove slopes sufficiently shallow that the entire sloping wall is composed of a step train with intervening terraces of the facet orientation. The analysis here is for evolution by evaporation–condensation processes and should also apply to the junction between a grain boundary and a crystal–melt interface in an isothermal, single-component system.

If the grain boundary free energy is γ_b and the surface free energy of the solid–vapor interface is γ , then it is energetically favorable for a groove to form at the grain boundary when $\gamma_b < 2\gamma$. The corresponding dihedral angle 2θ at the base of the groove is given by $\gamma_b/2\gamma = \cos \theta$ (e.g., Ref. 17). The groove deepens and widens with time, and the shape profile smoothly varies (in the continuum limit) until it intersects the planar surface; see Fig. 1. Traditionally, uses of solutions of the grooving problem include comparing them with experiments in order to extract estimates for surface diffusion coefficients¹⁸ and features of the surface energy.^{6,19}

Two limits of the grooving of a grain boundary have been studied, and numerous extensions have been offered for surface processes above the roughening temperature. In the first limit, surface evolution occurs by evaporation–condensation processes, and the surface profile $h(x,t)$ follows from $v_n = \zeta(\mu - \mu_0)$, where μ is the local chemical potential of the surface, μ_0 is a reference value of the vapor, v_n

^{a)}Electronic mail: has@deas.harvard.edu

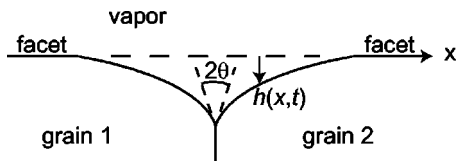


FIG. 1. The evolution of a grain boundary. Basic notation is indicated.

is the local normal velocity of a point on the interface, and $\zeta > 0$ is the surface mobility. Then, $\mu - \mu_0$ is proportional to the curvature of the interface, κ , with a proportionality coefficient related to the surface free energy. The description of the grain-boundary evolution is then completed by prescribing the dihedral angle 2θ at the base of the groove.

In the classical treatment by Mullins,⁴ the surface energy is assumed isotropic and constant, and the mobility is also assumed to be constant, in which case the resulting problem can be analyzed simply. For the one-dimensional configuration there is a similarity solution for the surface shape: $h(x,t) = t^{1/2}H(\eta)$, where the similarity variable η is proportional to $x/t^{1/2}$, which thus establishes the basic form of the surface evolution. We note that this similarity solution does not depend on a small-slope approximation. From this result we see that both the groove depth and width grow as the square root of time. The similarity function $H(\eta)$ is known analytically when the governing equation is linear;⁴ otherwise, a numerical solution to an ordinary differential equation (ODE) is necessary¹⁷ (see also Sec. II A). As we shall see in this paper, since below the roughening transition the surface energy is a nonanalytic function of the surface orientation (or slope), a new approach is necessary. Perhaps surprisingly, useful analytical approximations are obtained nevertheless.

In the second limit, the surface evolution can be driven by surface diffusion, in which case shape changes in time are proportional to the divergence of a surface current, which itself is proportional to the gradient of the chemical potential. For the classical case⁴ and with constant transport coefficients, $v_n \propto \nabla^2 \kappa$. This description of evolution, when combined with a grain-boundary condition involving surface slope, gives rise to a similarity solution $h(x,t) = t^{1/4}H(\eta)$, where now the similarity variable η is proportional to $x/t^{1/4}$; the form of this solution does not depend on a small-slope approximation. As before, the similarity function $H(\eta)$ is known analytically when the governing ODE is linear; otherwise, a numerical solution is necessary.

For temperatures below the roughening transition T_R the chemical potential differs from its classical form because of the nonanalyticity of the surface free energy as a function of the surface slope.¹⁶ Additionally, the surface mobility also may depend on the surface slope. In a microscopic picture, surface evolution is driven by step motion, and facets may develop where the step separation diverges to become macroscopic. We model the evolution of the entire morphology, including that of the facet, using a continuum description of the free-boundary problem.^{14,15,20} In particular, here we analyze the dynamics of grooving for the case of evaporation–condensation-driven evolution below the roughening temperature, $T < T_R$. As in the case of $T > T_R$, summarized

above, it is possible below T_R to construct a similarity solution of the form $h(x,t) = t^{1/2}H(\eta)$, where η is a similarity variable proportional to $x/t^{1/2}$ and $H(\eta)$ satisfies a nonlinear ODE. Although the problem is nonlinear, we shall show that an approximate analytical description is possible, from which we extract a relation between the groove width and the dihedral angle. A calculation of the surface-diffusion-driven evolution of a groove below the roughening temperature is given in Ref. 21.

II. THE EVOLUTION OF A GROOVE

A. A brief review of grooving above the roughening transition

We first describe the time-dependent formation of a groove that forms at a grain boundary of an otherwise flat surface (see Fig. 1) for the case that the evolution corresponds to dynamics above the roughening temperature. We let the one-dimensional groove profile be denoted by $h(x,t)$, which satisfies the nonlinear PDE¹⁷

$$\frac{\partial h}{\partial t} = \zeta_0 \gamma \frac{\partial^2 h / \partial x^2}{1 + (\partial h / \partial x)^2}, \quad (1)$$

where ζ_0 is the constant surface mobility and γ is the isotropic and constant surface free energy.

It is thus necessary to solve (1) subject to the condition $\partial h / \partial x(0,t) = -\cot \theta$, where θ is half of the dihedral angle. This problem admits a similarity solution of the form

$$h(x,t) = (2\zeta_0 \gamma t)^{1/2} H(\eta), \quad \text{with } \eta = \frac{x}{(2\zeta_0 \gamma t)^{1/2}}, \quad (2)$$

where $H(\eta)$ satisfies the nonlinear ODE

$$\left(H - \eta \frac{dH}{d\eta} \right) \left[1 + \left(\frac{dH}{d\eta} \right)^2 \right] = \frac{d^2 H}{d\eta^2}. \quad (3)$$

A numerical solution of (3) is necessary and is constructed by a procedure of guessing $H(0)$ with a given $dH/d\eta$ at $\eta = 0$ and shooting until $H(\eta \rightarrow \infty) \rightarrow 0$ (e.g., Ref. 17). For the special case of small surface slopes, Eq. (3) can be linearized, in which case the solution is

$$H(\eta) = \frac{\cos \theta}{\sin \theta} \left[\sqrt{2/\pi} e^{-\eta^2/2} - \eta \operatorname{erfc}(\eta/\sqrt{2}) \right], \quad (4)$$

where $\operatorname{erfc}(s) = (2/\sqrt{\pi}) \int_s^\infty e^{-\lambda^2} d\lambda$ is the complementary error function. Therefore, the groove deepens according to $h(0,t) = (4\zeta_0 \gamma t / \pi)^{1/2} \cot \theta$; the groove also widens at a rate proportional to $t^{1/2}$.

B. General formulation for grooving below the roughening transition

For a one-dimensional profile $h(x,t)$ below the roughening transition (see Fig. 1), we take as the surface free energy G per unit area projected on the basal plane a common form that arises from elastic dipole–dipole or entropic step–step repulsive interactions,²²

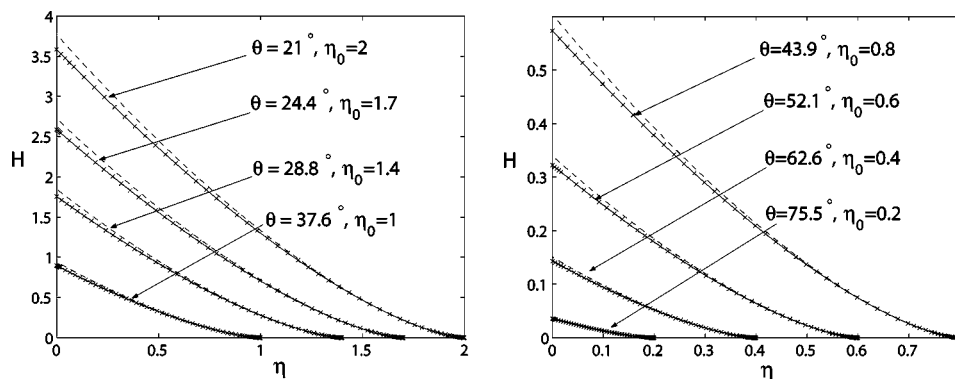


FIG. 2. The normalized groove shape $H(\eta)$ for grooving below the roughening transition with $\alpha=2$. The dashed curve is one term of the approximate solution (13), while the crosses represent the sum of the first two terms. The solid curve is the numerical solution of the nonlinear ODE (11).

$$G\left(\frac{\partial h}{\partial x}\right) = g_0 + g_1 \left| \frac{\partial h}{\partial x} \right| + \frac{1}{3} g_3 \left| \frac{\partial h}{\partial x} \right|^3, \quad (5)$$

where g_0 is the free energy of the terrace, g_1 is the step line tension, and g_3 is the strength of step-step interactions. In this case the local surface chemical potential, relative to the chemical potential of the vapor μ_0 , takes the form⁹

$$\mu - \mu_0 = -2g_3\Omega \left| \frac{\partial h}{\partial x} \right| \frac{\partial^2 h}{\partial x^2}, \quad (6)$$

where Ω is the atomic volume. In deriving (6) from (5) we assume that $\partial h/\partial x$ has not changed sign. Although g_1 does not appear in the chemical potential (6), since the steps are straight and parallel to the junction between the grain boundary and the vapor, the determination of the dihedral angle involves g_1 .

If adatoms emitted from steps desorb into the vapor after traveling a characteristic distance that is small compared to the step spacing, which is the usual case, the rate of interface motion is proportional to the step density. For small deviations from equilibrium, the surface evolution is described by²⁰⁻²³

$$\frac{\partial h}{\partial t} = -k \left| \frac{\partial h}{\partial x} \right|^b (\mu - \mu_0), \quad (7)$$

where k is a constant and $b=1$. Alternatively, if adatoms emitted from surface steps rapidly coat the neighboring terraces before desorbing into the vapor, then the step density is no longer a factor in (7) and $b=0$. Combining Eqs. (6) and (7) leads to the nonlinear PDE

$$\frac{\partial h}{\partial t} = \beta \left| \frac{\partial h}{\partial x} \right|^\alpha \frac{\partial^2 h}{\partial x^2}, \quad (8)$$

where $\beta=2kg_3\Omega$ and $\alpha=b+1$. Below we consider two cases for α , $\alpha=1$ and $\alpha=2$.

At the grain boundary, $x=0$, we have the boundary condition

$$\frac{\partial h}{\partial x}(x=0, t) = -\frac{\cos \theta}{\sin \theta}, \quad (9)$$

where 2θ is the dihedral angle. If there is local equilibrium in the immediate vicinity of the junction between the grain boundary and the surfaces, then the vanishing variation of the total surface energy with respect to junction position implies $\cos \theta = \gamma_b/2\gamma$ for two grains with mirror symmetry.²⁴ In

this case, the relation of γ to G , i.e., $\gamma = G/\sqrt{1+(\partial h/\partial x)^2}$, when combined with Eq. (5), is sufficient to relate the dihedral angle to the surface energies g_i . We also require h and $\frac{\partial h}{\partial x} \rightarrow 0$ as $|x| \rightarrow \infty$, which, along with an initial condition, is sufficient to specify the surface evolution according to Eq. (8). Here we only need consider $x \geq 0$, which is the case of a groove with a symmetric profile. If the two grains have different surface energies then the grain boundary does not remain vertical; the treatment of such a problem is beyond the scope of the present work. Finally, note that the case $\alpha=0$ reduces (8) to the linearized limit of the classical problem of grooving above T_R . In the following we consider $\alpha > 0$.

The differential Eq. (8) and the boundary conditions can be satisfied for any α by the similarity solution

$$h(x, t) = (2\beta t)^{1/2} H(\eta), \quad \text{where } \eta = \frac{x}{(2\beta t)^{1/2}}. \quad (10)$$

Substitution into Eq. (8) yields the nonlinear ODE

$$H - \eta \frac{dH}{d\eta} = \left| \frac{dH}{d\eta} \right|^\alpha \frac{d^2 H}{d\eta^2} \quad (11)$$

with boundary conditions

$$\frac{dH}{d\eta}(0) = -\frac{\cos \theta}{\sin \theta} \quad \text{and} \quad H \rightarrow 0 \quad \text{as} \quad \eta \rightarrow \infty. \quad (12)$$

For mathematical details concerning the case with arbitrary positive α and the behavior of the solution, see the Appendix. We consider two representative cases for α next.

C. The slope-dependent surface mobility: $\alpha=2$

In the next two sections we provide numerical results for the nonlinear differential equation describing grooving below T_R , construct an approximate analytical solution, and show that the approximate solution is in remarkably good agreement with the numerical results. Hence, for all practical purposes the analytical results should be useful for those interested in detailed predictions.

Inspection of Eq. (11) shows that as $H \rightarrow 0$, then $H \propto (\eta_0 - \eta)^{3/2}$, where η_0 is the location where $H \equiv 0$; see the Appendix for details. This finite position where the groove ends is characteristic of nonlinear equations (here it is a consequence of the nonanalyticity of the surface free energy) and does not arise in more familiar, linear diffusion equa-

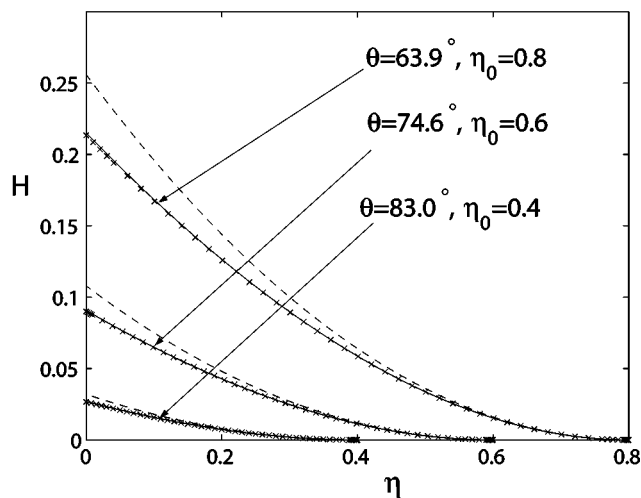
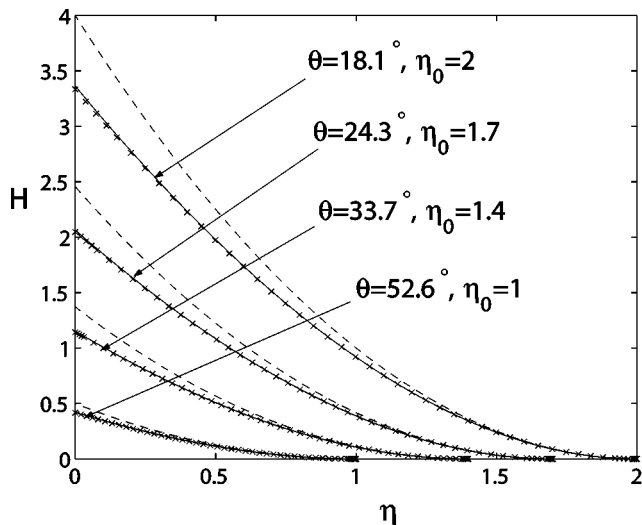


FIG. 3. The normalized groove shape $H(\eta)$ for grooving below the roughening transition with $\alpha=1$. The dashed curve is one term of the approximate solution (18), while the crosses represent the sum of the first two terms. The solid curve is the numerical solution of the nonlinear ODE (11).

tions. With this observation, it can then be shown that the solution near the “touch down” point η_0 has the expansion

$$H(\eta) = a_1(\eta_0 - \eta)^{3/2} + a_2(\eta_0 - \eta)^{5/2} + a_3(\eta_0 - \eta)^{7/2} + a_4(\eta_0 - \eta)^{9/2} + \dots \tag{13}$$

We assume that the surface forms a facet (flat region) for $\eta > \eta_0$, and $H(\eta)$ connects smoothly to the zero slope of the facet; see Fig. 1. From the general results given in the Appendix, Eqs. (A3a)–(A3d) with $\alpha=2$ yield

$$a_1 = \frac{2\sqrt{2}\eta_0}{3}, \quad a_2 = -\frac{1}{15\sqrt{2}\eta_0},$$

$$a_3 = \frac{1}{3780(2\eta_0)^{3/2}}, \quad a_4 = \frac{29}{68040(2\eta_0)^{5/2}}. \tag{14}$$

Conveniently, we can then numerically solve the ODE (11) by choosing a value of η_0 , integrating backwards until $\eta = 0$, and reading off the value of the slope at the origin, which identifies θ for the given value of η_0 . Also, Eq. (13), with the known values of the coefficients a_i , then serves as an approximate analytical solution.

Solutions for the surface profile $H(\eta)$ are shown in Fig. 2 for different values of η_0 and the corresponding value of θ . Numerical results to the nonlinear ODE are shown by the solid curves, the dotted line indicates one term of the analytical approximation (13), and the crosses result from using two terms of (13). We see that the two-term analytical approximation is in near perfect agreement with the numerical solutions.

The analytical representation of the solution (13), when evaluated at $\eta=0$, provides estimates for both the depth of the groove and the relation between η_0 and θ . Using just one term we first find, using the boundary condition (12), $\sqrt{2}\eta_0 = \cot \theta$ so that

$$H(0) = \frac{\sqrt{2}}{3} \cot^2 \theta. \tag{15}$$

Using two terms, we arrive at the slightly improved estimates

$$\eta_0 = \frac{12}{11\sqrt{2}} \cot \theta \text{ and } H(0) = \frac{228\sqrt{2}}{605} \cot^2 \theta. \tag{16}$$

With these results we can obtain an estimate for the time dependence of the groove depth:

$$h(0, t) = (2\beta t)^{1/2} \frac{228\sqrt{2}}{605} \cot^2 \theta, \tag{17}$$

which is distinct from the above roughening solution that has $h \propto \cot \theta$.

In addition, with the above results we have an explicit analytical relation between the groove width (in similarity variables) and the dihedral angle, $\eta_0 = (12/11\sqrt{2}) \cot \theta$, which corresponds to the actual groove width w varying as $w_{\alpha=2} = (12(\beta t)^{1/2}/11) \cot \theta$. Furthermore, the above results make clear that an excellent approximate analytical solution for all x and t is provided by combining Eqs. (10), (13), (14), and (16).

D. The slope-independent surface mobility: $\alpha=1$

We next consider the case where the surface evolves according to Eq. (11) with $\alpha=1$. We take the same approach as above to show that as $H \rightarrow 0$, then $H \propto (\eta_0 - \eta)^2$, where η_0 is the location where $H=0$. Thus, we take

$$H(\eta) = a_1(\eta_0 - \eta)^2 + a_2(\eta_0 - \eta)^3 + a_3(\eta_0 - \eta)^4 + a_4(\eta_0 - \eta)^5 + \dots, \tag{18}$$

where (A3a)–(A3d) with $\alpha=1$ yield

$$a_1 = \frac{\eta_0}{2}, \quad a_2 = -\frac{1}{12}, \quad a_3 = \frac{1}{288\eta_0}, \quad a_4 = \frac{1}{11\,520\eta_0^2}. \quad (19)$$

A numerical solution of (11) is generated by choosing η_0 , integrating backwards until $\eta=0$, and identifying the angle θ from the value of the slope at the origin.

Typical numerical results for the surface profile for different dihedral angles (2θ) are shown in Fig. 3. We observe that just two terms of the analytical approximation (18) are in excellent, in fact near perfect, agreement with the numerical solutions of the nonlinear ODE. One term of the analytical approximation yields $\eta_0 = (\cot \theta)^{1/2}$ and $H(0) = \frac{1}{2}(\cot \theta)^{3/2}$, while two terms yield the improved results $\eta_0 = (2/\sqrt{3})(\cot \theta)^{1/2}$ and $H(0) = (10/9\sqrt{3})(\cot \theta)^{3/2}$. Thus, for this version of the mobility function the groove depth varies in time according to

$$h(0,t) = (2\beta t)^{1/2} \frac{10}{9\sqrt{3}} (\cot \theta)^{3/2}. \quad (20)$$

The corresponding groove width is predicted to change in time as $w_{\alpha=1} = (8\beta t \cot \theta/3)^{1/2}$. In summary, we thus have found an excellent approximate solution for all x and t by combining the estimate for η_0 with Eqs. (10), (18), and (19), which effectively renders unnecessary the numerical solutions of the governing nonlinear PDE.

III. DISCUSSION

Perhaps surprisingly, for the case of grooving below the roughening temperature T_R , the similarity solution for the surface profile has the same scaling form (proportional to $t^{1/2}$) as the corresponding solution for the classical form, where $\mu - \mu_0$ is proportional to the local curvature. The details are, however, different above and below the roughening temperature and the functional dependence on the dihedral angle θ is different and dependent on the form of the surface mobility. It can, nevertheless, be recognized that the mathematical reason for the identical form of the time-dependent scaling follows from the basic transport equation, which has the form

$$\frac{\partial h}{\partial t} \propto f\left(\frac{\partial h}{\partial x}\right) \frac{\partial^2 h}{\partial x^2}, \quad (21)$$

where $f(\partial h/\partial x)$ is a function of the step density, with a boundary condition $\partial h/\partial x|_{x=0} = \text{constant}$. Equation (21), for any function f that depends only on the surface slope, and the boundary condition that also involves the slope, admits a similarity solution with $x \approx t^{1/2}$, from which the constraint on slope requires $h \propto t^{1/2}$.

We have shown that for two different forms of the surface mobility, $\alpha=1, 2$, analytical approximations of the nonlinear PDE describing surface grooving by evaporation–condensation processes below T_R are in near perfect agreement with the numerical solutions. These results should effectively negate the need in the future to solve these differential equations for the grooving problem below T_R . Finally, we have obtained explicit relations that illustrate the dependence of the groove depth and width on the dihedral

TABLE I. A summary of the main analytical results (exact or approximate).

α	$h(0,t)$	η_0 vs θ	width (w_α) vs θ
0^a	$\left(\frac{4\xi_0\gamma t}{\pi}\right)^{1/2} \cot \theta$...	$\propto (2\xi_0\gamma t)^{1/2}$
1	$(2\beta t)^{1/2} \frac{10}{9\sqrt{3}} (\cot \theta)^{3/2}$	$\frac{2}{\sqrt{3}} (\cot \theta)^{1/2}$	$\left(\frac{8\beta t \cot \theta}{3}\right)^{1/2}$
2	$(2\beta t)^{1/2} \frac{228\sqrt{2}}{605} (\cot \theta)^2$	$\frac{12}{11\sqrt{2}} \cot \theta$	$\frac{12(\beta t)^{1/2}}{11} \cot \theta$

^aThe results from a linearized analysis (see Sec. II A).

angle θ and the functional form of the surface mobility. The main mathematical results of this paper are conveniently summarized in Table I.

ACKNOWLEDGMENTS

We thank V. Shenoy and Z. Suo for helpful conversations. This research was supported by the Harvard NSEC (Grant No. NSF-PHY-0117795). M.J.A. was supported by the National Science Foundation (Grant No. DMR-0306997).

APPENDIX

In this Appendix we give some general results that relate to the analytical solution of the nonlinear ODE that arises in the description of grooving below T_R by evaporation–condensation processes. To begin with, we note that the solution of Eq. (11) depends on α . We require that $H \rightarrow 0$ as $\eta \rightarrow \eta_0$, where $0 \leq \eta < \eta_0$. By setting $H \sim \alpha_1(\eta_0 - \eta)^{\beta_1}$, $\beta_1 > 0$, we find $\beta_1 = 1 + 1/\alpha$:

$$H(\eta) \propto (\eta_0 - \eta)^{1+(1/\alpha)}. \quad (A1)$$

More generally, an expansion of the form

$$H(\eta) = a_1(\eta_0 - \eta)^{\beta_1} + a_2(\eta_0 - \eta)^{\beta_2} + a_3(\eta_0 - \eta)^{\beta_3} + \dots + a_j(\eta_0 - \eta)^{\beta_j} + \dots \quad (A2)$$

entails that $\beta_{j+1} = \beta_j + 1$ ($j=1, 2, \dots$). The coefficients a_j of the first four terms are calculated as functions of α and η_0 by substitution of (A2) into (11):

$$a_1 = \alpha \frac{(\eta_0 \alpha)^{1/\alpha}}{1 + \alpha}, \quad (A3a)$$

$$a_2 = -\frac{1}{2\eta_0} \frac{(\eta_0 \alpha) 1/\alpha}{(1 + \alpha)(1 + 2\alpha)}, \quad (A3b)$$

$$a_3 = \frac{1}{24\eta_0^2} \frac{-2\alpha^2 + 3\alpha + 3}{\alpha(1 + \alpha)^2(1 + 2\alpha)(1 + 3\alpha)} (\eta_0 \alpha)^{1/\alpha}, \quad (A3c)$$

$$a_4 = \frac{1}{48\eta_0^3\alpha^2} \frac{2\alpha^3 + 4\alpha^2 - \alpha - 1}{(1 + \alpha)^2(1 + 2\alpha)(1 + 3\alpha)(1 + 4\alpha)} (\eta_0\alpha)^{1/\alpha}. \quad (\text{A3d})$$

It should be borne in mind that η_0 depends only on α and θ because its value is found by applying (A2) near $\eta = \eta_0$ and integrating (11) to the origin where (12) is satisfied. Effectively, Eqs. (A2) and (A3) provide an analytical approximation to the solution of the nonlinear ODE (11) that characterizes the self-similar groove profile.

¹W. W. Mullins, *Acta Metall.* **6**, 414 (1958).

²H. J. Frost, C. V. Thompson, and D. T. Walton, *Acta Metall. Mater.* **38**, 1455 (1990).

³C. Lou and M. A. Player, *J. Phys. D* **35**, 1805 (2002).

⁴W. W. Mullins, *J. Appl. Phys.* **28**, 333 (1957).

⁵T. Xin and H. Wong, *Acta Mater.* **51**, 2305 (2003).

⁶W. Zhang, P. Sachenko, and I. Gladwell, *Acta Mater.* **52**, 107 (2004).

⁷H. P. Bonzel, E. Preuss, and B. Steffen, *Appl. Phys. A: Solids Surf.* **35**, 1 (1984).

⁸M. V. R. Murty, *Phys. Rev. B* **62**, 17004 (2000).

⁹A. Rettori and J. Villain, *J. Phys. (France)* **49**, 257 (1988).

¹⁰H. P. Bonzel and E. Preuss, *Surf. Sci.* **336**, 209 (1995).

¹¹A. Chame, S. Rousset, H. P. Bonzel, and J. Villain, *Bulg. Chem. Commun.* **29**, 398 (1996).

¹²N. Israeli and D. Kandel, *Phys. Rev. B* **62**, 13707 (2000).

¹³N. Israeli and D. Kandel, *Phys. Rev. Lett.* **88**, 116103 (2002).

¹⁴D. Margetis, M. J. Aziz, and H. A. Stone, *Phys. Rev. B* **69**, 041404 (2004).

¹⁵D. Margetis, M. J. Aziz, and H. A. Stone, *Phys. Rev. B* **71**, 165432 (2005).

¹⁶E. E. Gruber and W. W. Mullins, *J. Phys. Chem. Solids* **28**, 875 (1967).

¹⁷Z. Suo, *Adv. Appl. Mech.* **33**, 193 (1997).

¹⁸A. Tsoga and P. Nikolopoulos, *Acta Metall. Mater.* **41**, 1057 (1994).

¹⁹P. Sachenko, J. H. Schneibel, and W. Zhang, *Philos. Mag. A* **82**, 815 (2002).

²⁰H. Spohn, *J. Phys. I* **3**, 69 (1993).

²¹D. Margetis, M. J. Aziz, and H. A. Stone (unpublished).

²²H.-C. Jeong and E. D. Williams, *Surf. Sci. Rep.* **34**, 171 (1999).

²³A. Pimpinelli and J. Villain, *Physics of Crystal Growth* (Cambridge University Press, Cambridge, 1998).

²⁴C. Herring, in *The Physics of Powder Metallurgy*, edited by W. E. Kingston (McGraw-Hill, New York, 1951).